Lithium-Ion Batteries Hot Paper

DOI: 10.1002/ange.201307655

# A Lithium-Rich Compound $Li_7Mn(BO_3)_3$ Containing $Mn^{2+}$ in Tetrahedral Coordination: A Cathode Candidate for Lithium-Ion Batteries

*Semih Afyon, Michael Wörle, and Reinhard Nesper**

Four-coordinate $Mn^{2+}$ is a rare species owing to the lower ligand-field stabilization compared to the octahedral environment and—to our knowledge—was hitherto only reported with structure-directing multidentate ligands.[1] $Li^+$ ions tend to be octahedrally coordinated but may also appear in a tetrahedral environment, for example, in $Li_2O$. The title compound $Li_7Mn(BO_3)_3$ contains a relatively large fraction of cations where both $Li^+$ and $Mn^{2+}$ are in tetrahedral coordination environments with the exception of two Li sites. It can be written as $M^I{}_7M^{II}{}_1(M^{III}{}_3)O_9$ with M:O = 11:9 (where M = Li, Mn, B). In addition, there may be a structure-directing effect of the planar borate groups preventing a more-compact arrangement with higher coordination numbers. The peculiar tetrahedral environment of $Mn^{2+}$ could allow a wide range of oxidation-number switches without trapping specific states, such as octahedral $Mn^{4+}$. Together with its large concentration of Li atoms this compound could potentially become a fully lithiated cathode material for lithium-ion batteries, extending the limited range of electric vehicles.[2,3]

The presently employed $Li_x(Ni,Mn,Co)O_2$ (NMC) and $Li_xFePO_4$ (LFP) are quite moderate in terms of capacity with theoretical specific charges of 140 to 170 mA h g$^{-1}$.[4,5] The poor electronic conductor LFP, which can be activated by wrapping up nanoparticles in a conductive composite, has a high cycling stability which is ascribed to the linking phosphate groups. Borate groups may fulfill a similar function but at a lower specific weight. To exchange more charge per mass unit, several oxidation-state switches have to be realized at the redox-active cations, eventually reaching the high oxidation states of the transition metal center. Manganese is especially suited for this purpose. However, at high oxidation states monomeric units like the permanganate anion are formed, which easily dissolve in liquid electrolytes and thus induce battery failure. Herein, inert linker groups such as $BO_3$ units are used to solve part of the problem. The use of monoborates, such as $LiMBO_3$ (M = Fe, Mn, Co) as cathode materials for Li-ion batteries was first investigated by Legagneur et al. but only 4% and 2% Li were extractable for $LiFeBO_3$ and $LiMnBO_3$, respectively, owing to low ionic and electronic conductivities.[6] Yamada et al. obtained about 190 mA h g$^{-1}$ for $LiFeBO_3$, which is close to the theoretical specific capacity.[7] Recently, we demonstrated a high capacity of 145 mA h g$^{-1}$ within 4.7–1.7 V for h-$LiMnBO_3$ by employing nanoparticles and a composite electrode utilizing reduced graphite oxide.[8] Even though the theoretical capacities for $LiFeBO_3$ and $LiMnBO_3$, of approximately 220 and 222 mA h g$^{-1}$, respectively, are larger than those of presently employed oxides, capacities are still low compared to what in principle is possible and future needs.[9–11]

Herein, we present the new Li-rich compound $Li_7Mn(BO_3)_3$ which has been synthesized by thermalization of $Li_2O$, MnO, and $B_2O_3$ in exact stoichiometric amounts. The colorless crystals are of triclinic symmetry (space group $P\bar{1}$ (no. 2), *see* Experimental Section) and establish a new structure type. The crystal structure of $Li_7Mn(BO_3)_3$ (Figure 1) contains six crystallographically different $BO_3^{3-}$ ions ($d$(B-O) = 1.31–1.43 Å) of which only one is exclusively linked to $Li^+$ ions. All other borate units are linking two $Mn^{2+}$ ($d$(Mn-O) = 2.01–2.08 Å) and ten $Li^+$ ions in tetrahedral fashion ($d$(Li-O) = 1.87–2.21 Å). Within 3.3 Å there are no further oxygen neighbors around the Mn centers. Two Li sites have five close O neighbors with larger mean separation $d_{mean}$(Li-O) = 2.02 and 2.09 Å compared to $d_{mean}{}^{tetr}$(Li-O) = 1.976 Å and there are two three-coordinate $Li^+$ ions with $d_{mean}$(Li-O) = 1.92 and 1.93 Å. One belongs to a split position with two nearly equivalent closely neighboring sites while the other one has an additional far O neighbor at 2.49 Å. This arrangement is not surprising as there is considerable $Li^+$ mobility as found by our electrochemical investigations.

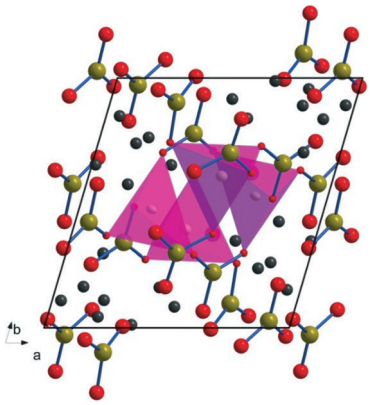


***Figure 1.*** View of the crystal structure of $Li_7Mn(BO_3)_3$ along [001] corresponding to the direction of columns of linked $MnO_4$ tetrahedra pairs (pink) interconnected by $BO_3^{3-}$ ions (B green, O red, Li black).

[*] Dr. S. Afyon, Dr. M. Wörle, Prof. Dr. R. Nesper
ETH Zurich, Department of Chemistry and Applied Biosciences
CH-8093 Zurich (Switzerland)
E-mail: nesper@inorg.chem.ethz.ch

Supporting information for this article is available on the WWW under http://dx.doi.org/10.1002/anie.201308655.

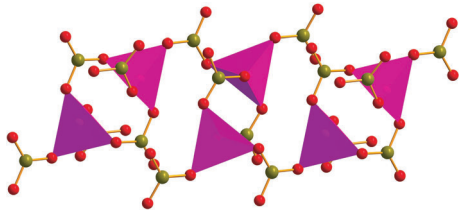

***Figure 2.*** Columns of pairs of $MnO_4$ tetrahedra (pink) interconnected by $BO_3^{3-}$ ions extending along the crystallographic *c*-axis showing one translational unit (B green, O red).

The $MnO_4$-tetrahedra form columns extending along the crystallographic *c*-axis (Figure 2) and only have Li atoms in their first coordination spheres. One of the $BO_3^{3-}$ units connects two of the tetrahedra in pairs and another one links the tetrahedra pairs in the columns. Terminal $BO_3^{3-}$ units provide the fourth oxygen atoms to the $MnO_4$-tetrahedra.

To our knowledge, the tetrahedral coordination of manganese in such a low oxidation state is unique compared to other $Mn^{2+}$ oxide compounds. Typically $MO_6$ octahedra or $MO_5$ (M = Fe, Mn, Co in $LiMBO_3$) polyhedra with trigonal bipyramidal or square-pyramidal geometry have been found.[6] This tetrahedral coordination may help to stabilize the borate–manganate framework up to higher oxidation states $Mn^{n+}$ with $n > 4$.

$Li_7Mn(BO_3)_3$ synthesized by thermalization occurs mainly in the form of 4–5 μ crystallites, along with sub-micron particles detected in scanning electron microscopy (SEM) images (see Figure 4a). Powder X-ray diffraction patterns for $Li_7Mn(BO_3)_3$ (Figure 3) show no reflections that could indicate any impurities. Figure 3c shows the XRD powder pattern of the nano-composite material that is obtained by ball-milling of crystalline $Li_7Mn(BO_3)_3$ (75 wt%) with carbon black (25 wt%). The broadening of diffraction peaks indicates the particle-size reduction of the pristine crystallites to the nanometer range. This finding is supported by electron microscopy images. After ball-milling with carbon black, the crystallite size has been reduced to 50–200 nm (Figure 4d). Nano-carbon particles disperse very well among the nano-crystallites (Figure 4d,e) and are embedded on the surfaces of particle agglomerates (Figure 4b,c) possibly enhancing the short- and long-range conductivity within the composite electrode. The presence of nano-carbon on the rims of particles is also evident from transmission electron microscopy images (Figure 4d,e, Supporting Information Figure S7).

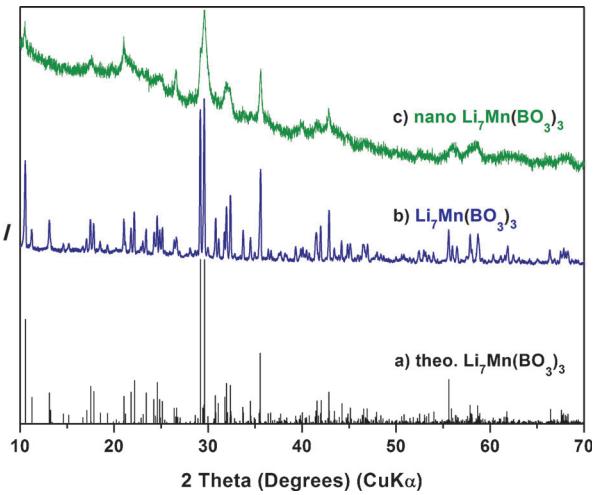


***Figure 3.*** Powder XRD patterns for $Li_7Mn(BO_3)_3$: a) theoretical, b) bulk crystalline, c) nano-composite.

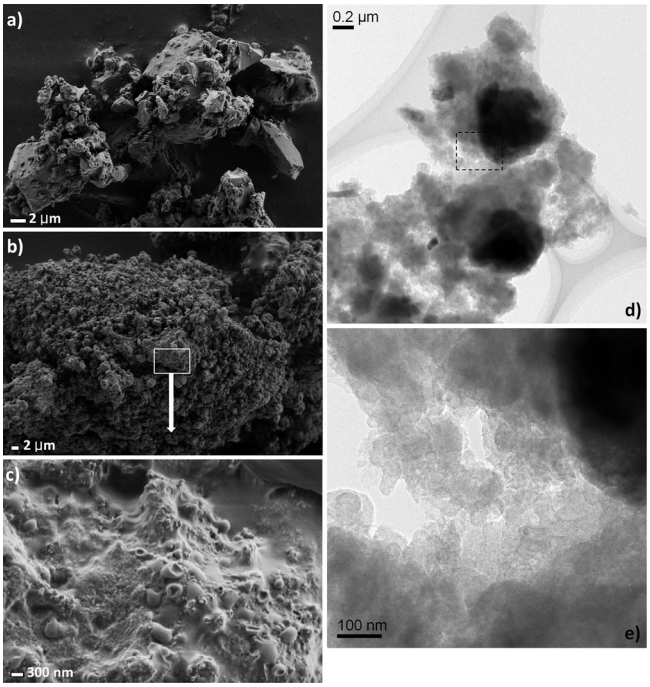


***Figure 4.*** Scanning electron micrographs (SEM) of a) bulk crystalline $Li_7Mn(BO_3)_3$, b) nano-composite of $Li_7Mn(BO_3)_3$, c) magnified image of the marked region in (b) showing carbon on the surface of particle agglomerates. Transmission electron micrographs (TEM) of d) nano-composite of $Li_7Mn(BO_3)_3$, e) enlarged image of the marked region in (d) showing the carbon black coverage of nano-crystallites.

Like related borates, $Li_7Mn(BO_3)_3$ has an intrinsically low electronic conductivity (ca. $10^{-11}$ S cm$^{-1}$) which is already indicated by its colorless crystals. Consequently, micron-sized crystalline $Li_7Mn(BO_3)_3$ is hardly electrochemically active with a first discharge capacity of about 10 mA h g$^{-1}$ within a potential window of 4.7–1.7 V at 10 mA g$^{-1}$ rate (Figure S5). This limited practical capacity with clear polarization is due to low conductivity. To gain a reasonable electrochemical activity, the utilization of nanoparticles and conductive coatings are required, similar to the cases of $LiMPO_4$ and $LiMBO_3$ (M = Fe, Mn, Co), where this has been shown to be crucial for activation.[7,8,12–14] However, $Li_7Mn(BO_3)_3$ has several prerequisites for a high energy density electrode material for Li-ion batteries: a high theoretical capacity of nearly 480 mA h g$^{-1}$ at an exchange of 5 Li per formula unit. With an average cell potential higher than 3 V against lithium metal, it could reach about 1500 W h kg$^{-1}$. Containing Mn in borate-linked tetrahedra may allow for a better stabilization of different oxidation states by help of the borate framework to counterbalance the large redox stress.

Comparable to related compounds, such as $LiMnBO_3$ and $LiFePO_4$, practical capacities were only reached and polarization widely diminished after preparing nano-composite electrodes of $Li_7Mn(BO_3)_3$ (ncLMB). The first galvanostatic charge/discharge curve for the ncLMB is presented in Figure 5a. The cell was cycled between 4.7 and 1.7 V at a rate of

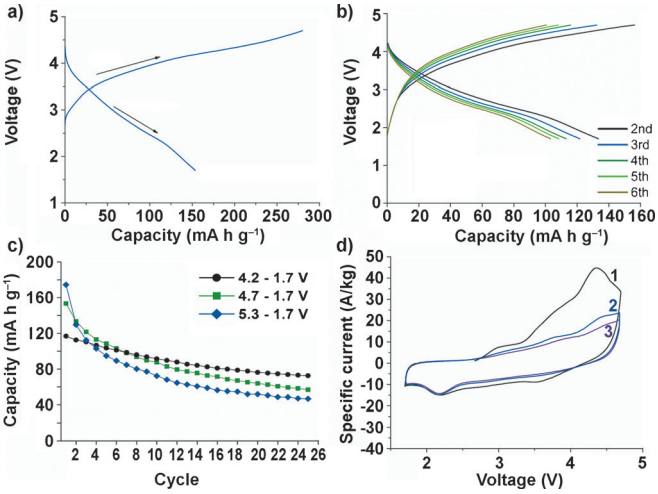


***Figure 5.*** Electrochemical tests for the nano-composite of $Li_7Mn(BO_3)_3$: a) the first charge/discharge curve within 4.7–1.7 V at 10 mA g$^{-1}$, b) subsequent charge/discharge curves, c) discharge capacity versus cycle number, d) cyclic voltammogram (cycles 1–3) between 4.7 and 1.7 V at a scanning rate of 0.05 mV s$^{-1}$.

10 mA g$^{-1}$ and it delivers a first charge capacity of about 280 mA h g$^{-1}$ corresponding to an extraction of approximately 3 Li per formula unit and a specific energy of around 1135 W h kg$^{-1}$. The first discharge capacity amounts to approximately 154 mA h g$^{-1}$ and charge/discharge capacities are reversible in subsequent cycles with an average discharge capacity loss of approximately 2.5% per cycle for the first 25 cycles (Figure 5c). The cyclic voltammogram of ncLMB is shown in Figure 5d. Broad oxidation and reduction peaks with marked polarization appear. The peak intensities for oxidation and reduction decrease at each cycle which is consistent with the capacity loss found in the galvanostatic measurements; however, the peak positions approximately remain unchanged which may be interpreted as reversible lithiation/delithiation mechanisms. In the first cycle the oxidation region shows up as three distinct effects at around 3.0 and 4.4 V, and a broader process around 3.3 to 4.1 V. The reduction starts at around 4.3 V with two reduction effects at around 3.6 and 2.2 V. The voltammogram enters into a smooth behavior in the subsequent cycles, and only the reduction effect at around 2.2 V remains distinct.

The irreversible capacity loss may have several sources, for example, amorphization of the electrode material, the formation of electrochemically inactive phases, contact losses owing to volume work and SEI (solid electrolyte interface) formation, respectively. X-ray powder patterns of the electrodes of ncLMB in the charged and discharged states provide evidence for partial amorphization during cycling as suggested by the broadening of diffraction peaks (Figure S6). However, formation of new crystalline phases or shifts of diffraction peaks between charged and discharged states were not detected.

Even ncLMB becomes amorphous upon cycling, it should be noted that amorphization is not necessarily a drawback but can even become favorable for electrode performance if transport properties and redox-activity are not impaired. Smaller losses were realized between 4.2–1.7 V than in the two larger potential ranges, which is further encouraging for the improvement of cycling properties and electrochemical performance of ncLMB (Figure 5c, and Figures S8, S9).

In conclusion, the new compound $Li_7Mn(BO_3)_3$ comprises a network of $MnO_4$ tetrahedra and $BO_3^{3-}$ units as characteristic structural features of a new structure type. It has $Mn^{2+}$ ions in tetrahedral coordination environments which is a unique situation compared to related manganese oxides. While micron sized crystals deliver a negligible first charge/discharge capacity, a high first charge capacity of approximately 280 mA h g$^{-1}$ (extraction of ca. 3 Li) and a first discharge capacity of approximately 154 mA h g$^{-1}$ were obtained after the conversion into nanoparticles and nanocarbon composite formation. Better electrochemical performance and cycling stability should be reachable by exploring new synthetic routes that may yield smaller nanoparticles, optimizing the conductive coatings on the surface of particles, improving the composites and better binding of the composites to prevent changes during lithiation/delithiation. If properly activated the compound may serve as a novel cathode material for Li-ion batteries giving distinctly increased energy density.

## Experimental Section

Crystals of $Li_7Mn(BO_3)_3$ were synthesized from high purity $Li_2O$ (99.5%, Alfa Aesar), MnO (99%, Sigma–Aldrich), and $B_2O_3$ (99.9%, Alfa Aesar) mixed in stoichiometric amounts and pressed into pellets in an Ar filled glove box. The pressed pellets were sealed in a Nb tube that is heated in a quartz tube under vacuum (ca. $10^{-1}$ mbar) at 850 °C for 24 h. After cooling to 700 °C at a rate of 10 °C h$^{-1}$, the sample was quenched to room temperature. The compound was also obtained in an open system with stoichiometric amounts of $Li_2CO_3$ (99.9%, Strem), MnO (99%, Sigma–Aldrich), and $H_3BO_3$ (99.9%, Acros) which were pressed into pellets, placed in a glassy carbon crucible with a lid, and annealed at 660–700 °C for 15 h under reductive CO atmosphere. Successive cooling, grinding, mixing and re-annealing of the reaction product yield high purity $Li_7Mn(BO_3)_3$. A nanocomposite electrode material was obtained by ball-milling of crystalline $Li_7Mn(BO_3)_3$ (75 wt%) with carbon black (Super P® Li Timcal) (25 wt%) under Ar atmosphere. The handling and electrode fabrication were carried out in a glove box, as the formation of $LiB(OH)_4$ occurs when this material is exposed to air for a few hours.

Electrochemical tests: Electrodes containing approximately (70 wt%) $Li_7Mn(BO_3)_3$, (20 wt%) conductive carbon (Super P® Li Timcal) and (10 wt%) polyvinylidene fluoride (PVDF) binder were prepared from a slurry with *N*-Methyl-2-pyrrolidone (NMP) that was cast on Ti current collectors and dried at approximately 100–120 °C under vacuum. The final electrodes consisted of approximately 6–7 mg active material. Li metal disks prepared from a 0.75 mm-thick ribbon (Aldrich) served as anode, and 1 M solution of $Li[(C_2F_5)_3PF_3]$ in EC:DMC (1:1) (Merck, LF-30 SelectiLyte) was used for the electrolyte, which is electrochemically stable within the voltage window employed. Swagelok cells were assembled in an Ar-filled glove box.

Galvanostatic measurements were carried out within 4.7–1.7 V at a rate of 10 mA $g^{-1}$, and within 4.2–1.7 V and 5.3–1.7 V at 10 mA $g^{-1}$ charge rate, 5 mA $g^{-1}$ discharge rate. The cyclic voltammetry was with a sweep rate of 0.05 mV $s^{-1}$ between 4.7 and 1.7 V.

Characterization: For structure determination, a crystal of $Li_7Mn(BO_3)_3$ of suitable size ($0.1 \times 0.18 \times 0.28$ mm) was selected under a microscope using polarized light. A data set was collected on a Bruker SMART CCD 1 K area detector diffractometer using MoKα-radiation (0.71073 Å). As the crystals are always twinned, the crystal structure had to be determined from a multiple twin. Further details for the solution and refinement of the structure are given in Supporting Information.

Crystal Data: $Li_7Mn(BO_3)_3$, $M_r = 279.95$, triclinic, $a = 8.3234(15)$, $b = 9.1952(17)$, $c = 11.248(2)$ Å, $\alpha = 71.495(4)$, $\beta = 79.525(4)$, $\gamma = 71.368(4)°$, $V = 770.5(2)$ Å$^3$, $T = 293$ K, space group $P\bar{1}$ (no. 2), $Z = 4$, $\rho_{calcd} = 2.413$ mg m$^{-1}$ m$^3$, $\mu$(MoKα) = 1.738 mm$^{-1}$, $wR_2 = 0.1721$ (all data) and $R_1 = 0.0537$ ($I > 2\sigma(I)$).Largest difference electron density peaks in the difference map are 0.85 and −1.00 e Å$^{-3}$, respectively.

Further details on the crystal structure investigations may be obtained from the Fachinformationszentrum Karlsruhe, 76344 Eggenstein-Leopoldshafen, Germany (fax: (+49) 7247-808-666; e-mail: crysdata@fiz-karlsruhe.de), on quoting the depository number CSD-425095.

Powder X-ray diffraction patterns were obtained on a STOE Stadi P diffractometer equipped with a germanium monochromator and $CuK_{\alpha 1}$ radiation (operated at 40 kV, 35 mA).

Scanning electron microscopy (SEM) was performed on a Zeiss Gemini 1530 operated at 1 kV, transmission electron microscopy (TEM) on a CM30ST (FEI; $LaB_6$ cathode) and a Tecnai F30 microscope that were operated at 300 kV with a maximum point resolution of ca. 2 Å.

Received: August 30, 2013
Published online: October 14, 2013

**Keywords:** borates · cathode material · lithium · lithium-ion batteries · manganese

[1] U. Olsher, R. M. Izatt, J. S. Bradshaw, N. K. Dalley, *Chem. Rev.* **1991**, *91*, 137 – 164.
[2] Mitsubishi-motors, Mitsubishi Innovative Electric Vehicle http://www.mitsubishi-motors.com/special/ev/, (May 2012).
[3] Nissan, Nissan Leaf Electric Car, http://www.nissan-global.com/EN/NISSAN/LEAF/, (May 2012).
[4] S. H. Jensen, K. Engelbrecht, C. Bernuy-Lopez, *J. Electrochem. Soc.* **2012**, *159*, A791 – A797.
[5] M. Safari, C. Delacourt, *J. Electrochem. Soc.* **2011**, *158*, A1123 – A1135.
[6] V. Legagneur, Y. An, A. Mosbah, R. Portal, A. L. La Salle, A. Verbaere, D. Guyomard, Y. Piffard, *Solid State Ionics* **2001**, *139*, 37 – 46.
[7] A. Yamada, N. Iwane, Y. Harada, S. Nishimura, Y. Koyama, I. Tanaka, *Adv. Mater.* **2010**, *22*, 3583.
[8] S. Afyon, D. Kundu, F. Krumeich, R. Nesper, *J. Power Sources* **2013**, *224*, 145 – 151.
[9] X. L. Ji, K. T. Lee, L. F. Nazar, *Nat. Mater.* **2009**, *8*, 500 – 506.
[10] P. G. Bruce, S. A. Freunberger, L. J. Hardwick, J. M. Tarascon, *Nat. Mater.* **2012**, *11*, 19 – 29.
[11] Z. Q. Peng, S. A. Freunberger, Y. H. Chen, P. G. Bruce, *Science* **2012**, *337*, 563 – 566.
[12] D. Lepage, C. Michot, G. X. Liang, M. Gauthier, S. B. Schougaard, *Angew. Chem.* **2011**, *123*, 7016 – 7019; *Angew. Chem. Int. Ed.* **2011**, *50*, 6884 – 6887.
[13] T. Drezen, N. H. Kwon, P. Bowen, I. Teerlinck, M. Isono, I. Exnar, *J. Power Sources* **2007**, *174*, 949 – 953.
[14] L. Y. Xing, M. Hu, Q. Tang, J. P. Wei, X. Qin, Z. Zhou, *Electrochim. Acta* **2012**, *59*, 172 – 178.